



Design of micro porous Al foams by high energy milling

M.H. Robert ^{a,*}, R.R. Silva ^b

^a Faculty of Mechanical Engineering, State University of Campinas, SP, Brazil

^b IFSP - Federal Institute of Education, Science and Technology, SP, Brazil

* Corresponding e-mail address: helena@fem.unicamp.br

ABSTRACT

Purpose: To explore a new route to produce metallic foams which results in a structure of closed micro porous. High energy milling is employed to incorporate particles of foaming agents in metallic powders to promote homogeneous distribution of micro gas bubbles during foaming.

Design/methodology/approach: AA2014 powders were mixed with TiH₂ particles as gas releasing agent, through high energy milling, producing composite powders. Powders were compacted and obtained compacted precursors were heated to promote foaming of the metal. Effect of processing conditions in the expansion of the metal, structural characteristics, density and mechanical properties under compression, of obtained foams was analyzed.

Findings: Foaming composite powders of AA2014/TiH₂ produced by high energy milling is a promising route to produce micro porous aluminium foams. The best foaming condition among the conditions investigated, occurs for the highest milling time (17 h) and highest heating rate (3°C/s) imposed during foaming, resulting in 140% of maximum expansion and foams with relative density of 0.44.

Research limitations/implications: Main limitation of the proposed process is the long time required to produce composite powders by high energy milling, which can justify the process for specific purposes where micro porous are required. However, as all new development, further works can lead to the optimization of processing parameters, mainly concerning reduction of processing time, to make the process compatible to wider industrial applications.

Practical implications: New products can be developed for specific applications requiring porous with micro scale.

Originality/value: The use of the foaming agent structurally incorporated in the metal powder to produce precursors for foaming is original.

Keywords: Cellular Material; Metallic Foams; Micro porous foams; High Energy Milling (HEM); AA 2014 foams

Reference to this paper should be given in the following way:

M.H. Robert, R.R. Silva, Design of micro porous Al foams by high energy milling, Archives of Materials Science and Engineering 71/1 (2015) 5-15.

MATERIALS

1. Introduction

Porous or cellular metals show specific combinations of properties such as high absorption of energy during plastic deformation in impact situations, damping properties, thermal and acoustic insulation, among others, associated with low density. These characteristics make metallic foams or sponges suitable for many different applications; foams, which present voids as closed cells, find utilization mainly as low weight structural materials, while sponges or open cell foams find main application as functional materials for filters, heat exchangers, etc., as well reported in the literature [1-5]. Particularly, aluminium foams have been increasingly applied in the building and transport industry, specially automotive and aeronautical fields [6,7].

Many distinct processes have already been developed to produce aluminium and other metallic foams; processing routes are usually classified in two major groups: direct and indirect foaming of liquid metal. Direct foaming is related to the promotion of gas bubbles in the liquid by means of direct injection of air or inert gases, or generated by foaming agents, products that deliver gases by chemical reactions such as dissociation at high temperatures. In the production of foams of aluminium and its alloys, TiH_2 is the most conventional foaming agent employed [8,9]. This hydride dissociates at around 450°C delivering H_2 gas to the liquid metal.

Most popular indirect routes make use of powder technology techniques. The preparation of a foamable precursor from mixed and compacted powders of the metal alloy and the gas deliver agent is required; the precursor is heated to a high temperature to promote liquid formation and the expansion of gases to result in closed cells in the metallic structure [10-12].

The physics of foaming a liquid metal can involve complex phenomena and the success of a foaming process depends on their understanding and control, in particular the aspects related to the stabilization of the bubbles. Gases tend to float and escape to the atmosphere, to blow near the free metal surface as liquid drainage by gravity weakens the bubbles surface, to collapse as the metal pressure overcome the superficial tension, to suffer coalescence as they approach etc. [13,14]. Addition of solid particles to the liquid, such as SiC in aluminium alloys, helps to promote bubbles stability due to increase in the melt viscosity and attachment to the bubbles surface preventing their contact.

Properties of metal foams are strongly dependent on the density of the material and the architecture of the spatial arrangement of voids and metallic walls. Furthermore, structure of the metallic cell walls also plays its role in the

foam mechanical behaviour. These features depend on the process employed to produce the foam; different fabrication techniques result in cells presenting different geometry, distribution and dimensions.

Most of the aluminium foamed products in the market for different structural purposes present spherical voids in the range of 1-10 mm. Porous dimensions depend on the size and distribution of the particle of the foaming agent and the stability of the individual gas bubble generated in the liquid.

When using PM route for the manufacturing of closed-cell foams, distribution of the metal and the foaming agent powders in the mixture is a crucial issue, once bad dispersion of the gas releasing agent can lead to irregular pores distribution in the foam product. Searching for alternative way to improve particles of foaming agent distribution in the mixture, this work investigates the effect of using high energy during the milling stage of metal and foaming agent powders. High energy milling (HEM) shall promote entrapment of the foaming agent particles in the metal matrix, which actually must turn to a composite powder [15,16]. A fine dispersion of particles is expected, which, associated with some probable improvement in compacting the mixture, can result in fine, dispersed porous in the foamed product.

Therefore, the main goal of this work is to explore a new alternative to produce aluminium foams with fine, micro scale porosity, based on HEM techniques.

2. Experimental procedures

Figure 1 shows schematic representation of the investigated route to produce foams with micro scale porous. Atomized powder of the alloy AA2014, with chemical composition according to Table 1, was used in the experiments. Figure 2 shows general aspect of the powder particles and their microstructure.

Table 1.
Chemical composition of the AA2014 powder used (%wt).

Cu	Si	Mg	Fe	Ca	Ti	Mn	Ni	Al
4.39	0.38	0.28	0.08	0.02	0.01	0.01	0.01	bal.

The AA2014 powder particles are approximately globular, with average diameter around 20 μm ; density of 2.78 g/cm^3 and micro hardness of 83 ± 10 HV. Microstructure is typical of atomized powders, presenting fine dendritic alpha phase and fine eutectic constituent in boundaries.

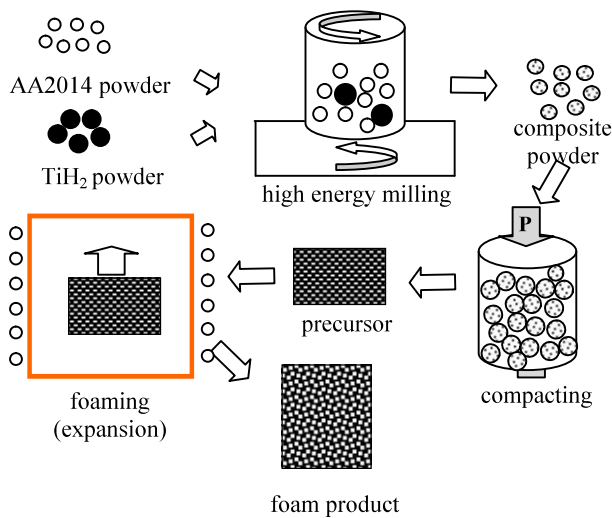


Fig. 1. Schematic representation of the processing route proposed to produce aluminium foams with micro porous

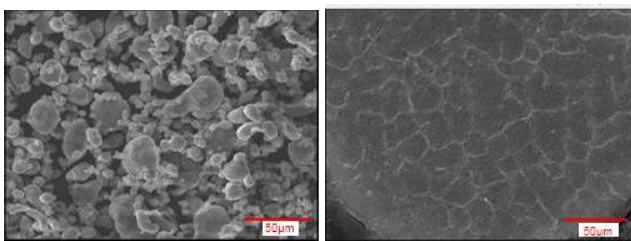


Fig. 2. General aspect and microstructure of the AA2014 powder particles used in the experiments (SEM)

Titanium di-hydrate TiH₂ was used as foaming agent; particles present irregular polygonal morphology, as shown in Fig. 3, with average size around 42 µm; density of 4.14 g/cm³ and micro hardness of 227 ± 86 HV.

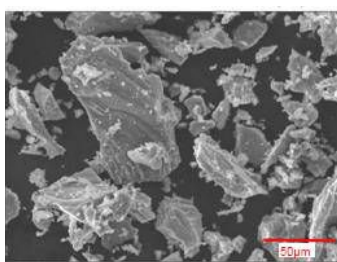


Fig. 3. General aspect of the TiH₂ powder particles used as foaming agent (SEM)

Results of thermo gravimetric tests show decomposition of TiH₂ starting around 440°C, with relatively low mass

loss up to 560°C, and significant mass loss from this temperature up to 635°C. Generated H₂ gas acts as foaming agent in the liquid.

Pre-mixtures of AA2014 alloy and TiH₂ (1.5 wt%) powders were milled using planetary ball mill under the conditions: Cr-steel balls with balls/charge ratio 6:1; speed 650 rpm; milling times of 1, 5, 9, 13, 15 and 17 h. Stearic acid (1.5 wt%) was used as process controlling agent (PCA). After milling, powder mixtures were submitted to uniaxial double compression: at 200°C using 300 MPa, followed by second compression at 400°C and 300 MPa. Resulting compacted precursors were heated to promote foaming, at two different rates: 1 and 3°C/s. Uniaxial expansion was forced by inserting precursor samples in a quartz cylinder open at the top surface. Expansion behaviour was recorded with a camera; after maximum expansion was reached, products were cooled in air.

Density measurements of the final products were performed in a He gas picnometer; microstructure of cell walls in the foams was observed by optical and electronic microscopy in samples prepared using conventional metallography techniques. Mechanical behaviour under compression was evaluated in semi-static tests.

3. Results and discussions

3.1. Milling step: composite powders produced

Figure 4 shows general aspect of the AA2014/TiH₂ powders under different milling times; microstructure of the particles are shown in Fig. 5. As pointed previously, hardness of the powders that constitute the mixture greatly differs: TiH₂ particles are circa 3x harder than AA2014 particles; therefore during milling ductile aluminium powder is expected to undergo heavy plastic deformation while fragile TiH₂ must suffer fracture. As observed in Fig. 4, increasing milling time promotes strong modification in the morphology and size of the particles involved. For the shortest time (1 h), already some change is noticed, as more flat particles are present; after 5 h it is possible to observe drastic deformation of the aluminium powder, which present now clear lamellar morphology. This characteristic and the microstructure can be better observed in Fig. 5: lamellar aluminium particles tend to aggregate, in a welding process, leaving lines of oxide among layers. At the milling time of 9 h, welding of lamellar particles is more effective and tendency to get spherical morphology is noticed. After 13 h, particles present more globular and homogeneous morphology and smaller general dimensions.

As well known in high energy milling, ductile particles are severely deformed and fracture can occur, this effect opposing the welding process of lamellas stimulated by the breakdown of oxide layers in the powder particles surface. The overall effect in the size of particles is therefore dependent on the supremacy of one effect over the other. In the results shown, from 9 h onwards of milling, mechanisms of fracture seem to be dominant over the welding process, since particles have their size reduced. Powders obtained after 15 and 17 h of milling present morphology nearly equiaxial; the smallest dimensions are obtained for 17 h.

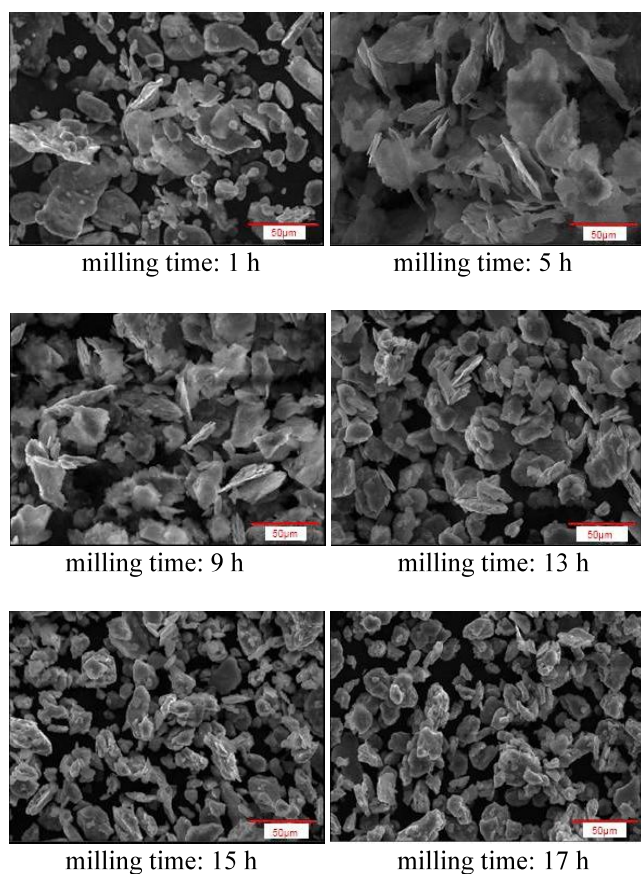


Fig. 4. General aspect of mixtures AA2014/TiH₂ powders under different milling times (SEM)

Microstructures observed in Fig. 5 show that for 13 h onwards of milling, welding lines are less apparent, as the oxide films tend to disappear by fracture, distributing the oxides as small particles in the matrix.

Therefore, milling process promoted significant change in particles dimensions. Generally speaking, the resulting powder particles show decreasing dimensions as milling time increases, in the milling time range investigated. For

the shortest time (1 h) used in the experiments, average diameter of resulted particles is 104 ± 2 mm, while for the longest milling time (17 h) is 44 ± 2 mm. As there were no significant modifications from 15 to 17 h of milling, no experiments were made beyond this limit. Excessive milling time, besides the possibility of increasing particles dimensions, which could be prejudicial to the compression of the powders and the precursor porosity, is not interesting as far as overall processing time and energy input is concerned.

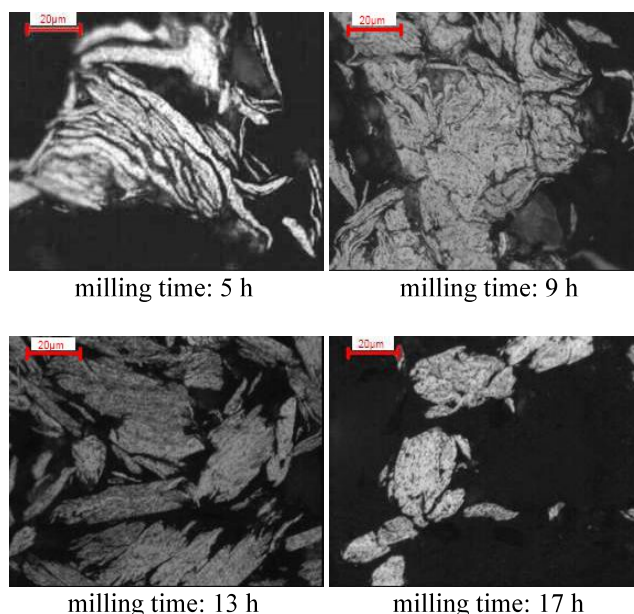


Fig. 5. Microstructures of AA2014/TiH₂ powders under different milling times (SEM)

Regarding the milling effect over the TiH₂ particles, some typical microstructures of powders for different milling times are presented in more detail in Fig. 6. After 1 h milling, TiH₂ particles are already entrapped among Aluminium particles, their size was reduced from the initial value of around 40 μm to a final 8 μm. As these particles present high hardness, fracture rather than deformation is expected during milling. The smaller, fractured particles of TiH₂ tend to be located at the welding lines of the lamellar aluminium powder. For longer milling times, TiH₂ particles get smaller (around 1 μm and even smaller) and are located more homogeneously dispersed throughout the aluminium matrix, as observed after 9 h of milling. Further increase in milling time does not seem to promote sensible effect in the size and distribution of TiH₂ particles in the aluminium matrix, as observed in the powder milled for 17 h.

As a general result of the milling process, best distribution of the foaming agent and best microstructure in the resulting composite powder are achieved after 17 h of milling.

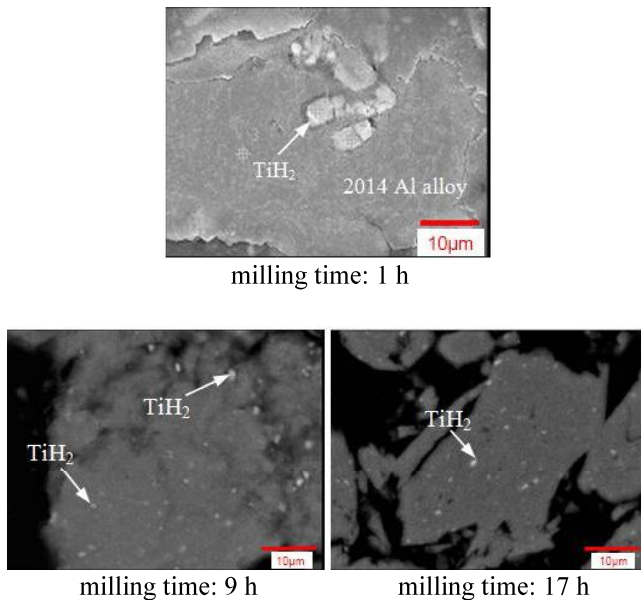


Fig. 6. Microstructures of AA2014/TiH₂ powder under different milling times: small TiH₂ located in the AA2014 structure (SEM)

The severe particles deformation during milling with high energy, associated with the incorporation of TiH₂ micro particles in the matrix, causes increase in the hardness of the resulted powder: it was observed variation of the hardness from 83 ± 10 HV (original aluminium powders) to 179 ± 18 HV, after 17 h of milling.

3.2. Compacting step: precursors

Composite AA2014/TiH₂ powders obtained by high energy milling were compacted to produce precursors for foaming. Results for powders milled for 9 and 17 h are presented here; these specific conditions are chosen as they represent different conditions in the powders structure in different steps of the milling process. In the first case, morphology of aluminium particles is less rounded and dimensions are bigger than in the second case, as described previously; while TiH₂ particles are similar in both cases. Besides, hardness of the particles are also distinct: average values are 156 ± 10 and 179 ± 18 respectively, as

consequence of more severe plastic deformation in the particles milled for longer time, as observed previously.

Results concerning density of green compacts show values of 2.74 ± 0.05 g/cm³ and 2.73 ± 0.02 g/cm³ for precursors produced from powders milled for 9 and 17 h, respectively. Although the supposed higher difficulty to compact the globular, harder particles of the powder produced by 17 h milling than the softer, more lamellar powder resulted after milling for 9 h, density values can't be differentiated. Differently of the usual significant influence of milling time on the compacting ability and resulting density of green compacts produced from powders presenting high ductility, like pure aluminium or AA6061 alloy, as reported, for example, by Fogagnolo [17], the influence of milling time in the compactability of AA2014 powders seemed not to be so significant, in the range analyzed.

3.3. Expansion step: foaming process

Selected precursors of similar densities were heated at two different heating rates to promote foaming. Typical results of temperature vs time and expansion vs time and temperature during foaming are presented in Fig. 7.

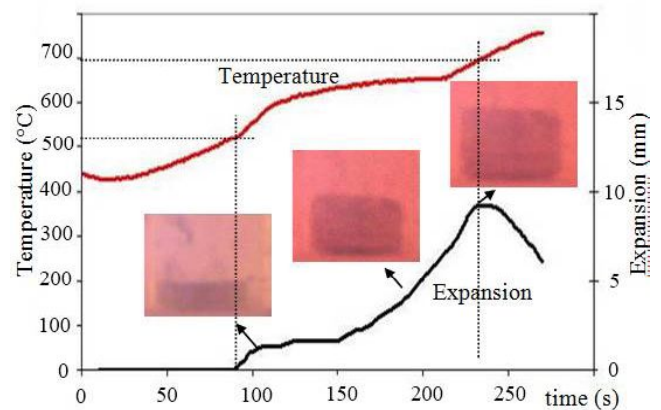


Fig. 7. Temperature vs time and expansion vs time during foaming of precursors of composite AA2014/TiH₂ powders milled for 17 h. Heating rate: 3°C/s

Temperature vs time curve shows the solidification range of the alloy around 600 and 680°C. In the expansion vs time curve it can be observed that expansion starts slowly around 510°C, accelerates in the solidification range of the metal (at low rate for small liquid fraction,

increasing rate as liquid fraction increases), and has its maximum around 700°C.

Similar behaviour of curves is obtained for the lowest heating rate investigated (1°C/s); obviously time to start expansion decreases and expansion rate increases as faster kinetics of foaming is imposed under the higher heating rate. Anyway, foaming process is very quick in both heating rates used in the experiments. Total expansion must be tightly controlled to prevent gas bubbles agglomeration and coalescence, escaping to the liquid surface, as well as excessive liquid drainage.

Some general results of expansion during foaming process are presented in Fig. 8 and Table 2.

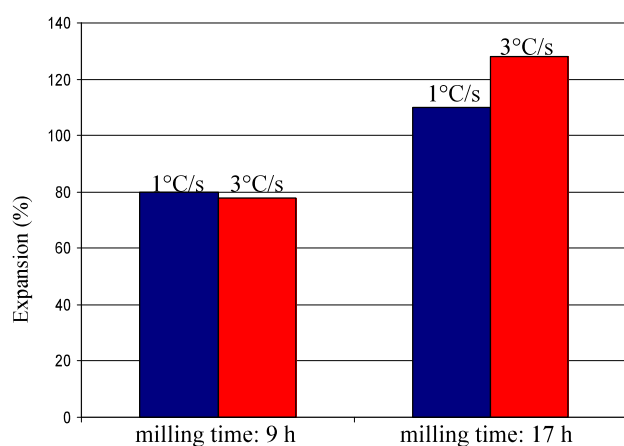


Fig. 8. General results of expansion vs foaming conditions of precursors of AA2014 / TiH₂; precursors produced from powders milled for different times

Table 2.

Data related to the foaming process of precursors of AA2014/TiH₂ composite powders obtained in different conditions

Milling time	¹ HR	² E _{max} (%)	³ T E _{max} (°C)	⁴ ER (%/s)
9 h	1°C/s	80 ± 9	693 ± 10	0.25 ± 0.02
	3°C/s	78 ± 15	721 ± 10	0.30 ± 0.07
17 h	1°C/s	110 ± 15	701 ± 12	0.37 ± 0.07
	3°C/s	128 ± 10	710 ± 5	0.52 ± 0.07

¹HR: Heating Rate; ²E_{max}: Maximum Expansion;

³T E_{max}: Temperature of Maximum Expansion;

⁴ER: Expansion Rate (linearized).

General results show average maximum expansion in the range of 80 to 130%; the first value is not so attractive but values from 100% are appealing for foaming processing. Due to the significant variation of values of maximum expansion-results show average values of 3 samples foamed in the same condition-effect of foaming parameters must be analysed here with care. While the effect of milling time clearly indicates increasing expansion with increasing milling time, the effect of heating rate in the expansion only a tendency can be inferred from the obtained data: for samples submitted to 9 h of milling, maximum expansion doesn't seem to be dependent on heating rate; while for powders milled for 17 h, increasing heating rate seems to cause some increasing in expansion.

To analyse the effect of milling time in the maximum expansion, it is necessary to have in mind the effect of this parameter in the structure of the powders. For 9 h of milling, as shown previously, powders are irregular, welding of deformed layers are not completed and oxides lines are still present; after compacting, total porosity of precursor is due to voids among particles plus voids inside the particles along the oxide layers. Probably the contribution of the porosity among particles to the total porosity is lower than the internal porosity, as the powder is easily compactable, as observed previously. As TiH₂ particles are located in the internal oxide lines among Aluminium layers, during foaming H₂ can escape easily first trough those lines (interfaces among layered, not welded particles) and then trough the porosity among agglomerates of aluminium powders.

For 17 h of milling, powders present more globular and homogeneous morphology, as welding of deformed layers is complete; therefore, less or shorter oxide lines are present to allow H₂ to escape trough. As TiH₂ is entrapped in the aluminium structure during foaming, retention of the gas is improved. Therefore, as higher contribution to the porosity of precursor made from powders submitted to 17 of milling is the inter particles porosity, loss in H₂ is lower, resulting in higher expansion.

This positive effect seems to compensate the fact that powders submitted to longer milling times are less compactable than powders milled for shorter times, which could lead to higher porosity due to voids among powder particles.

As a general result, it was observed that, although density of precursors are similar for both type of powders, distribution of porosity in the structure is vital for expansion: powders milled for shorter time are less expandable due to higher ability of gases to escape using

interfaces of oxide layers as escaping route. Concerning the effect of heating rate, it can be observed that expansion is fast for all situations, with average rate values varying from around 0.25 to 0.52%/s. However, the influence of porosity distribution is also crucial: it can be observed negligible effect of heating rate in the expansion in the case of powders milled for 9 h; on the other hand expansion of structures with less escaping route for the generated gas is more dependent on the heating rate imposed: increasing heating rate can prevent gas escaping, increasing total expansion, as observed.

Average temperature of maximum expansion lies from 690°C to 720°C, i.e., in liquid metal. Foaming temperature should be related only to the nature of the foaming agent, but some differences in the temperature for maximum expansion can be expected as foaming conditions change. Indeed, it can be observed some tendency of higher temperature for maximum expansion when using higher heating rate; in this case, gases can be prevented of escaping in early stages of the heating.

The best foaming condition among conditions investigated, occurs for the highest milling time and highest heating rate, resulting in 140% of maximum expansion. Improvements are probably possible by increasing density of precursors.

As the general results showed sensitivity of foaming parameters on the success of the process and moreover, the effect of processing parameters are interrelated, higher number of experiments allowed a statistical approach to build maps of correlating interferences. Figure 9 shows maps of expansion vs porosity of precursor and heating rate. General results show strong influence of milling time (it meaning distribution of porosity in the precursor) in the viability of the foaming process.

Considering 80% of expansion as the minimal acceptable in a foaming process, it can be observed that for precursors obtained from powders milled for 9 h, acceptable expansion is reached only if porosity in the precursor is lower than 2.0%. Only in a narrow processing window it is possible to achieve expansion in the order of 100%; this expansion requiring high heating rates and very low porosity in the compacted precursor.

When higher milling time is employed, results in map in Fig. 9 show expansion higher than 90% in any condition tested, independent on the heating rate, even for precursors with 3.25% of porosity. Therefore, porosity of precursor is less critical for the success of the foaming when using powders milled for longer time; process is more flexible and less sensible to foaming conditions in this case. Maps show a wide processing window to obtain expansions higher than 130%; even a reasonable processing window to achieve expansion higher than 160%.

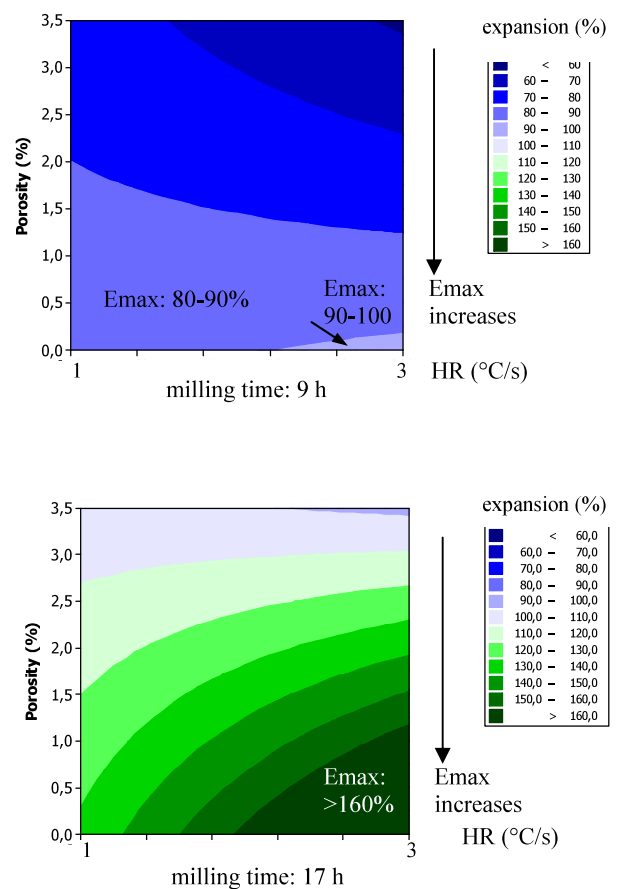


Fig. 9. Maps of expansion vs foaming conditions of precursors of AA2014/TiH₂; precursors produced from powders milled for different times

3.4. Foamed products

Figure 10 shows typical structures of foam products manufactured in conditions to produce maximum expansion, i. e., using the higher tested rating rate. Figure 10 (1) show general view of porous in products obtained from powders submitted to different milling times: it can be observed large amount of porous in both cases, but morphology, dimensions and distribution are distinct. Porous with elongated morphology are present in the foam produced from powders milled for 9 h, while porous with lower dimensions and less elongated are present in foams obtained from powders milled for 17 h present. Dimensions of porous can vary from a few microns to 540 μm in the first case and to 340 μm in the second case.

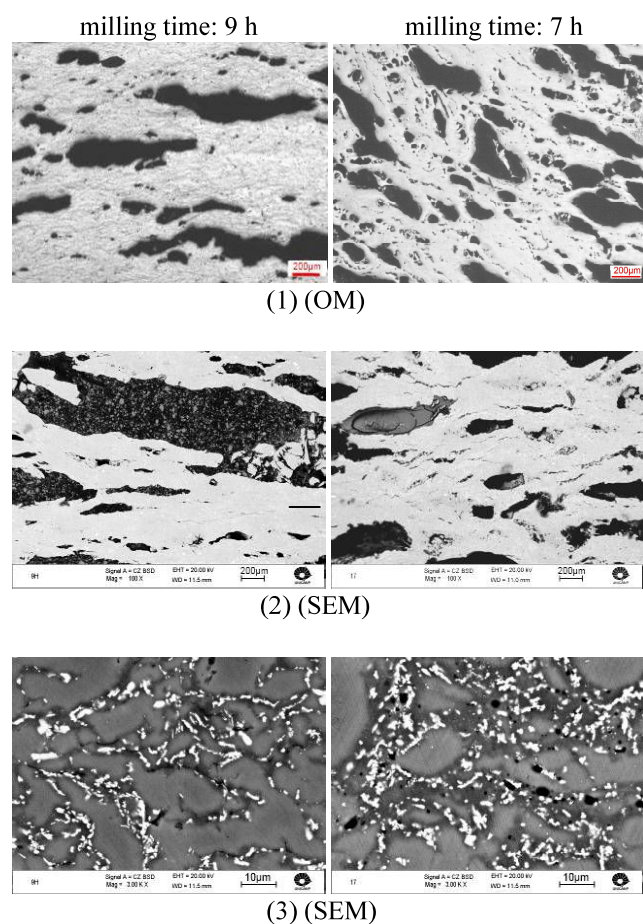


Fig. 10. Typical structures of AA2014 foams produced from powders milled for 9 and 17 h. Heating rate: 3°C/s

These results are accordingly with the internal structure of the powders in the precursors: as discussed previously, long lines of oxide are still present in the structure of the powder milled for the shorter time, while higher milling time is able to break and distribute the oxide layers in the metal structure. As the foaming agent particles are distributed along these lines, during foaming the gas can expand through the interface oxide/metal, resulting in long, lamellar porous in the first case and more rounded, lower dimension and better distribution, in the second case. Photos in Fig. 10 (2) show clearly the presence of long oxide lines in powders milled for 9 h and shorter, broken oxide lines in powders milled for 17 h.

Figure 10 (3) show microstructures of the metallic walls: it can be observed fine primary α phase with irregular morphology and coarse boundaries of eutectic phase. As the material was submitted to temperatures higher than T_{solidus} of the alloy, the H_2 gas could expand

through the liquid phase and eventually escape through oxide lines, as discussed, or be entrapped forming rounded, small porous, as observed in some cases.

On cooling, the liquid constituent solidifies as eutectic, with high segregation of Cu in the α phase and fine $CuAl_2$ particles. Some globularization of the primary α phase should be expected, but it was not so significant due to the short residence time within the solidification range.

Densities of produced foams in different conditions are presented in Table 3. In all cases, significant reduction in the density of the material was achieved, with relative values around 0.44 to 0.65 (density of bulk AA2014 alloy: 2.87 g/cm³). Concerning the effect of processing parameters, results show sensible influence of milling time of the powders in the density of the foamed product: higher milling time leads to lower density or higher porosity, due to higher retention of the H_2 gas in the structure, as discussed earlier. On the other hand, the effect of heating rate on the density is not so strong; however, it can be observed a tendency of decreasing density with increase in heating rate, as in this case acceleration of the foaming improves gas retention in the structure.

Table 3. Density and porosity of AA2014 foams produced from powders milled for 9 or 17 h (heating rate during foaming: 3°C/s)

Milling time of powders	¹ HR	Foam density (g/cm ³)	Foam relative density	Foam porosity (%)
9 h	1°C/s	1.87±0.20	0.65±0.07	35±7
	3°C/s	1.72±0.26	0.60±0.09	40±9
17 h	1°C/s	1.38±0.13	0.48±0.04	52±4
	3°C/s	1.27±0.06	0.44±0.02	56±2

¹HR: heating rate

Foamed products were submitted to compressive tests under semi-static load. Results of stress vs strain curves for samples with different densities are presented in Fig. 11.

Typical stress vs strain curves for cellular metals present basically three stages related to the material behaviour: elastic deformation for low stresses; a generally wide plateau of plastic deformation where strain increases significantly with low changes in the applied stress, and a final step where further plastic deformation requires higher increase in applied stresses. During the plateau of high deformation at low and practically constant stresses porous or cells are collapsed promoting the densification of the material. Further deformation requires higher stresses once

metallic walls are in contact and the metal behaviour is imposed.

Results shown in Fig. 11 for the produced foams show, in all cases, high plastic deformation under low stresses; however due to the high relative density comparing to typical porous materials, no flat plateau of plastic deformation is present, unlike macro porous cellular Al foams in the market. On the other hand, the small dimensions of cells in the micro porous material provides more regular plateau than in the case of Al foams with macro porous, which usually presents oscillations in the stress vs strain curves in this region, attributed to successive relieve of stress as individual cells collapse.

General results show clearly the influence of the foam density in its behaviour: deformation decreases and required stresses increase as density increases. Density seems to be the predominant parameter; further studies shall clarify the contribution of the influence of porous shape and distribution, as well as of the characteristics of the cell walls structure, presence of oxide layers, etc. which are related to the milling time, in the compressive behaviour of the foams.

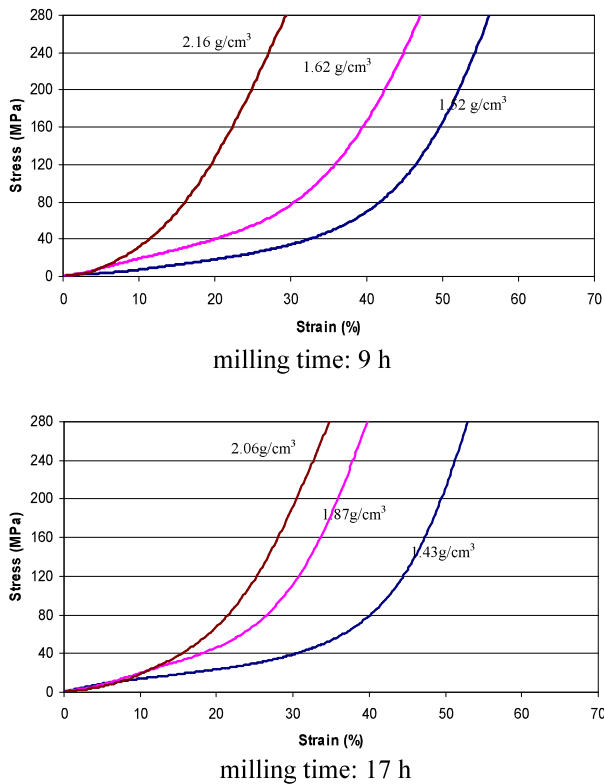


Fig. 11. Mechanical behaviour in compression, of AA2014 foams produced from powders submitted to high energy milling for different times. Density of samples as indicated

Some characteristics of the foams behaviour under semi-static compression where evaluated from stress vs strain curves using the model indicated in Fig. 12.

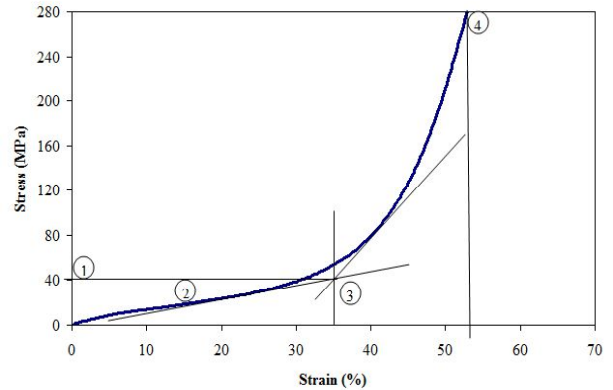


Fig. 12. Illustration of measurements of some characteristics of compression behaviour of the produced foams: point 1 - maximum stress in the plateau; point 3 - maximum strain in the plateau; point 4 - maximum strain; line 2 - linearization of the stress in the plateau

Tests were interrupted at 280 MPa to avoid complete smash of the specimen. Average stress in the plateau is the mean value from point 0 to point 1. It was not possible to calculate Young's modulus and yield strength due to the difficulty to determine the limit of the elastic regime in the stress vs strain curves.

General quantitative results obtained are presented in Table 4; values are approximate, due to the difficulty of the precise determination of inflexion points in the curves.

Table 4.

Approximate results on compressive characteristics of AA2014 foams produced from powders submitted to high energy milling

Milling time	Foam density (g/cm ³)	Plateau average stress (MPa)	Plateau max stress (MPa)	Plateau max strain (%)	Max strain at 280 MPa (%)
9 h	1.52	22	45	38	56
	1.62	37	70	32	47
	2.16	35	83	17	29
17 h	1.43	25	40	36	53
	1.87	26	51	23	40
	2.06	32	57	22	35

It can be observed in all cases high plastic deformation, varying from minimum 17 to maximum 38%, at very low

stresses, in the order of 22 to 36 MPa, due to collapse of cell walls, before curves get steeper in the last stage of the deformation. Values of total deformation are also quite significant, varying from circa 30 to 56%. The properties of aluminium foam produced by milled powders are strongly dependent on the density of the foam: low density values lead to higher deformation in the plateau and also final maximum deformation (examples 9 hs - 1.52 g/cm³ with 38% strain; and 17 hs - 1.43 g/cm³ with 36% strain). The average stress in the plateau and maximum stress in the plateau region increases with increasing density: for example, the values of average stress in plateau region ranged from approximately 25 MPa (lower density) to 32 MPa (higher density) for samples produced from powders milled for 17 h.

The general behaviour of the produced foams with micro porous is slighter poorer than general behaviour of commercial aluminium foams with the same density but presenting macro porous [18,19], as far as foams compressibility is concerned: micro porous foams are less deformable and requires higher stresses to collapse. Further studies shall clarify the contribution of different parameters to this behaviour: sizes and distribution of porous (and, as consequence, the thickness of cell walls among porous), and the condition of the structure of the metallic walls (fine and highly deformed in the case of 17 h milled powders and as cast in the case of conventional liquid foaming or even foaming of compacted precursors obtained by conventional milling of powders).

4. Conclusions

High energy milling showed to be a promising process to produce foams of Al alloys with micro porous. Porous in the order of 340 to 540 μm could be obtained by foaming compacted precursors of composite powders of AA2014 alloy with fine dispersion of the foaming agent TiH₂, produced by high energy milling. Among the different conditions tested, it can be concluded, concerning the effect of parameters in the foaming process: expansion during foaming increases with increasing milling time from 9 to 17 h; the effect of heating rate in the expansion shows a tendency of increasing expansion with increasing heating rate; lower density in the precursor leads to higher gas escaping and therefore low expansion.

Concerning the product characteristics, results showed that foams produced from powders submitted to short milling time present long lamellar porous while more roundish, lower dimension and better distribution of porous

is a tendency when milling time is increased. Foams with relative densities from 0.44 to 0.68 were obtained; higher milling time leads to lower density.

The mechanical behaviour of the foams with micro porous under compression is strongly dependent on the material density. Low densities lead to higher deformation under lower stresses in the plateau. The micro porous foams showed more stable plateau regime and very low elastic deformation; plastic regime can start very quickly, which could be good for applications in mechanical energy absorption.

Overall best results were obtained in the conditions: 17 h of milling and heating rate during foaming 3°C/s.

Acknowledgements

The authors want to thank financial support from the Brazilian Government Agencies: CAPES and CNPq National Council for Scientific and Technological Development.

Additional information

Selected issues related to this paper are planned to be presented at the 22nd Winter International Scientific Conference on Achievements in Mechanical and Materials Engineering Winter-AMME'2015 in the framework of the Bidisciplinary Occasional Scientific Session BOSS'2015 celebrating the 10th anniversary of the foundation of the Association of Computational Materials Science and Surface Engineering and the World Academy of Materials and Manufacturing Engineering and of the foundation of the Worldwide Journal of Achievements in Materials and Manufacturing Engineering.

References

- [1] T. Hipke, J. Hohlfeld, S. Rybandt, Functionally Aluminum Foam Composites for Building Industry, *Procedia Materials Science* 4 (2014) 133-138.
- [2] R. Nowosielski, A. Kania, M. Spilka, Development of ecomaterials and materials technology, *Journal of Achievements in Materials and Manufacturing Engineering* 21 (2007) 27-30.
- [3] J.A. Reglero, E. Solorzano, M.A. Rodriguez-Perez, J.A. de Saja, Design and testing of an energy absorber prototype based on aluminum foams, *Materials & Design* 31 (2010) 1-6.

- [4] A. Leonov, Cellular structure for catalysts and filters, *Met Foam*, Berlin - Germany, 2003, 47-50.
- [5] J. Banhart, Aluminium foams for lighter vehicles, *International Journal of Vehicle Design* 37 (2005) 114-125.
- [6] W. Azzi, W.L. Roberts, A. Rabiei, A study on pressure drop and heat transfer in open cell metal foams for jet engine applications, *Materials & Design* 28 (2007) 569-574.
- [7] J.A. Reglero, M.A. Rodríguez-Pérez, E. Solórzano, J.A. de Saja, Aluminium foams as a filler for leading edges: Improvements in the mechanical behaviour under bird strike impact tests, *Materials & Design* 32 (2011) 907-910.
- [8] A. Byakova, Y. Bezim'yanny, S. Gnyloskurenko, Takashi Nakamura, Fabrication Method for Closed-cell Aluminium Foam with Improved Sound Absorption Ability, *Procedia Materials Science* 4 (2014) 9-14.
- [9] T. Fukui, Y. Nonaka, S. Suzuki, Fabrication of Al-Cu-Mg Alloy Foams Using Mg as Thickener through Melt Route and Reinforcement of Cell Walls by Heat Treatment, *Procedia Materials Science* 4 (2014) 33-37.
- [10] M. Shiomi, S. Imagama, K. Osakada, R. Matsumoto, Fabrication of aluminium foams from powder by hot extrusion and foaming, *Journal of Materials Processing Technology* 210 (2010) 1203-1208.
- [11] L. Orovčík, M. Nosko, P.Š. Sr., Š. Nagy, M. Čavojský, F. Šimančík, J. Jerz, Effect of the TiH₂ pre-treatment on the energy absorption ability of 6061 aluminium alloy foam, *Materials Letters* 148 (2015) 82-85.
- [12] I. Duarte, M. Oliveira. Aluminium alloys foams: Production and Properties Powder Metallurgy, *Intech Rijeka* (2012) 47-72.
- [13] N. Babcsán, J. Banhart, D. Leitmeier, Metal foams-manufacture and physics of foaming, Hahn-Meitner Institute, Berlin, Germany, ARC Leicht metallkompetenzzentrum Ranshofen GmbH, Austria, 2005.
- [14] V. Gergely, T.W. Clyne Drainage in standing liquid metal foams: modelling and experimental observations, *Acta Materialia* 52 (2004) 3047-3058.
- [15] L.A. Dobrzański, M. Kremzer, M. Adamiak, The influence of reinforcement shape on wear behaviour of aluminium matrix composite materials, *Journal of Achievements in Materials and Manufacturing Engineering* 42 (2010) 26-32.
- [16] W. Pilarczyk, R. Nowosielski, A. Pilarczyk, P. Sakiewicz, A production attempt of Ni50Ti50 and Ni52Ti41Nb7 alloys by mechanical alloying method, *Archives of Materials Science and Engineering* 47/1 (2011) 19-26.
- [17] J.B. Fogagnolo, M.H. Robert, J.M. Torralba, Mechanically alloyed AlN particle reinforced Al 6061 matrix composites: Powder processing, consolidation and mechanical strength and hardness of as-extruded materials, *Materials Science and Engineering A* 426 (2006) 85-94.
- [18] S. Esmaeelzadeh, A. Simchi, D. Lehmhus, Effect of ceramic particle addition on the foaming behavior, cell structure and mechanical properties of P/M AlSi7 foam, *Materials Science and Engineering A* 424 (2006) 290-299.
- [19] D.P. Papadopoulos, I.Ch. Konstantinidis, N. Papanastasiou, S. Skolianos, H. Lefakis, D.N. Tshipas, Mechanical properties of Al metal foams, *Materials Letters* 58 (2004) 2574-2578.